

Strain analysis using deformed quartz veins

Análisis de la deformación a partir de venas de cuarzo

E. Druguet and A. Griera

Departament de Geologia, Universitat Autònoma de Barcelona. 08193 Bellaterra (Barcelona)
e-mail: geotec@geologia.uab.es

ABSTRACT

A detailed strain analysis of structures developed in anisotropic rocks from the Cap de Creus area is made using deformed quartz veins. Data on stretch of differently oriented veins allow to calculate the best-fit ellipsoids for different localities applying the minimum squared method. The results show that regional deformation in this area involved NW-SE shortening, with area loss in the horizontal section, and vertical extension. Structural and rheological controls are suggested to explain the partitioning of deformation inferred from this analysis.

RESUMEN

Se ha realizado un análisis detallado de la deformación en rocas anisótropas del Cap de Creus mediante el uso de venas de cuarzo deformadas. A partir de las medidas de la elongación de venas con diferentes orientaciones se han calculado, para distintas localidades, los elipsoides de deformación de mejor ajuste, aplicando el método de mínimos cuadrados. Los resultados muestran que la deformación en esta zona implicó un acortamiento en la dirección NW-SE, con reducción de área en la sección horizontal, y extensión vertical. Se sugiere que la partición de la deformación observada a partir de este análisis fue controlada por factores estructurales y reológicos.

Key words: strain analysis, deformed veins, finite strain ellipsoids, Cap de Creus.

Geogaceta, 24 (1998), 119-122
ISSN: 0213683X

Introduction

Stretch recorded by dykes and veins in ductily deformed rocks represent an useful tool to characterize the finite strain in two and three dimensions and, moreover, it has relevance in kinematic analysis of shear zones. These markers, especially quartz veins, have been commonly used for strain analysis (e. g. Talbot 1970, Hutton 1982, Ramsay 1967, Passchier 1990, Talbot and Sokoutis 1995). The present work shows a detailed strain analysis of structures associated to deep-seated deformation and metamorphism. Sets of differently oriented quartz veins allow to determine the stretch associated to folding and/or boudinage of each vein or segment of vein and, thus, they permit a quantitative estimation of the finite strain ellipsoids for multiple localities. Average values of finite deformation can be achieved from the integration of the results obtained from different outcrops.

Geological setting and structural pattern

The Culip area is located in the northeast Cap de Creus peninsula in NE Spain (Fig. 1), which forms the most easterly outcrop of Hercynian basement exposed along the Axial Zone of the Pyrenees. Two main lithological groups can be distinguished in the Cap de Creus peninsula: (i) a metasedimentary sequence and (ii) Hercynian granodiorite stocks. The rocks of the metasedimentary sequence are affected by a low pressure regional Hercynian metamorphism with grade increasing from the chlorite-muscovite zone in the south to the sillimanite zone in the north. The Hercynian in the Cap de Creus peninsula is complex and is characterized by polyphasic structures. Three main deformational events have been distinguished (Druguet 1997). The early event (D_1) developed a penetrative schistosity (S_1). The D_2 event produced

NE-SW to E-W trending steep folds that heterogeneously affected the S_1 schistosity in prograde metamorphic conditions. Progressive heterogeneous deformation at retrograde conditions produced NW-SE-trending D_3 folds and shear zones with associated mylonitic bands (Carreras and Casas 1987).

The Culip area is an illustrative example of heterogeneous D_2 deformation. The outcropping rocks correspond to the metasedimentary sequence consisting of an alternance of metapsammites and subordinate metapelites, and some thin layers of light quartzites. The area is located in the medium- to high-grade metamorphic zone, mainly formed by sillimanite-bearing micaschists, although andalusite is still present. A strain gradient across the area defines, in horizontal view, a shear zone-like geometry, with two main structural zones of relatively high and low strain (Fig. 1). Increase in strain is manifested by the increasing tightness of

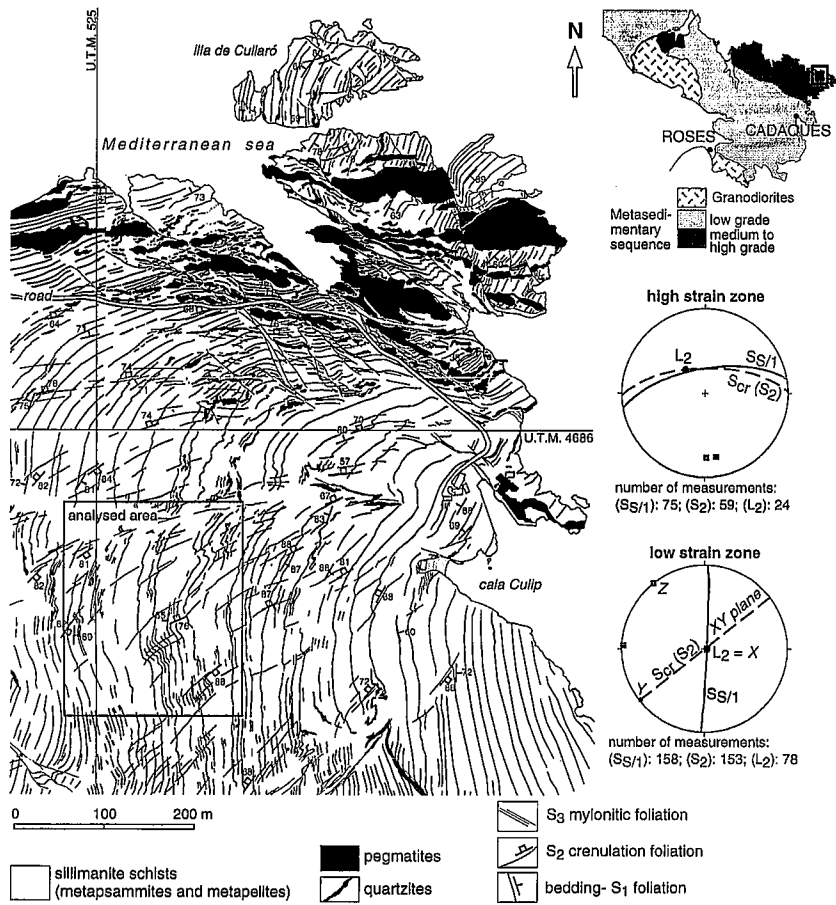


Fig. 1- Structural map of the Culp area in the NE Cap de Creus peninsula (Druguet 1997, modified), showing the location of the analysed area, and lower-hemisphere stereoplots. Mean great circles of S_1 (solid) and S_2 (dashed) and their poles (squares) are shown. L_2 = mean values of fold axes and stretching lineations. X, Y and Z = principal finite strain axes.

Fig. 1- Mapa estructural del área de Culp en el NE de la península del Cap de Creus (Druguet 1997, modificado), con la situación del área de estudio, y proyección estereográfica (hemisferio inferior). Los estereogramas indican los valores medios para los planos S_1 (en trazo continuo) y S_2 (en trazo discontinuo) y sus polos (cuadrados). L_2 = orientación media para los ejes de pliegues y lineaciones de estiramiento. X, Y y Z = ejes principales de la deformación finita.

folds and the clockwise rotation of both S_1 and S_2 foliations, leading to the sub-parallelism of both foliations in the high strain zone. High strain deformation is also associated to the syntectonic emplacement of a pegmatite dyke swarm (Carreras and Druguet 1994).

The present study considers the D_2 deformational features in the low strain zone. The structural pattern in this zone is rather homogeneous and characterized by a sub-vertical nearly N-S trending S_1 foliation, sub-parallel to bedding, which will be labelled $S_{s/1}$. In this domain, D_2 folding produces open «S»-shaped cylindrical folds in $S_{s/1}$, on a 10 cm-100 m scale. Associated to these folds, a NE-SW trending sub-vertical crenulation cleavage (S_2) develops preferentially in pelitic schists. Porphyroblasts of cordierite and andalusite, grown over S_1 , systematically

display an anti-clockwise rotation (in horizontal views) due to D_2 deformation.

Quartz segregation veins are abundant in the study area (Fig. 2). They are between few mm and few cm wide, with variable lengths, and have predominantly a sub-vertical attitude. Two main groups of quartz veins have been distinguished according to their space occurrence and relative time of formation. A first set, labelled Q1, consist of pre- D_1 veins (Fig. 2a). They are sub-parallel to bedding and some of them were boudinaged during D_1 event. These earlier boudinaged quartz veins are folded during D_2 , showing, as in the case of porphyroblasts, an anti-clockwise rotation of boudins. The second group, labelled Q2, includes sets of differently oriented veins which generally cross-cut the $S_{s/1}$ fabric (Fig. 2b and 2c). These Q2 veins are folded and/or boudinaged by D_2

depending of their orientation, although folded veins are more frequent. A change in orientation and an increase in fold tightness have been observed in many Q2 veins when passing from psammitic into pelitic layers. Folds are also tighter in Q1 veins within pelitic layers. These facts suggest that there might be a rheological control on veins deformation. Both schists and quartz veins show various orders of fold size: decametric, metric and cm-mm (Fig. 1, 2 and 3).

The D_2 folds have sub-vertical or steeply plunging axes, which are closely parallel to lineations. Lineations are usually stretching lineations defined by the alignment of quartz grains or mineral lineations defined by sillimanite, tourmaline or biotite. These lineations are developed in both the quartz veins and the bedding surfaces, and indicates that the X axis of the finite D_2 strain is sub-vertical. The described geometric relationships (steep $S_{s/1}$ and S_2 foliations, and sub-vertical fold axes and stretching lineations) imply that most features such folds, boudinage and asymmetric structures are better marked in flat-lying outcrop surfaces than in steep ones, i. e. the vorticity axis has a sub-vertical attitude (Fig. 3). The deduced orientation of the X, Y and Z principal axes of the finite strain ellipsoid is given in Fig. 1.

A structural and kinematic model for the Culp area and vicinities have been previously presented by Carreras and Druguet (1994), Druguet (1997) and Druguet *et al.* (1997). The whole structure is interpreted as a complex transpressive shear zone involving vertical extension, NNW-SSE subhorizontal bulk shortening with a dextral component, and bedding- S_1 parallel sinistral flexural flow.

Procedure for the strain analysis

We have selected the squared area in Fig. 1 in the low strain domain because of the abundance of quartz veins and because in higher strain domains the transposition of all earlier structures into a closely parallel trend prevents their use in strain analysis. Data on stretch values (S_1) and orientations (ϕ_1 , ϕ_2) of quartz veins have been taken from 80 different localities. Each locality shows a rather homogeneous deformation, with constant orientation of S_1 and S_2 foliations. A total number of 590 segments of quartz veins have been measured.

We have chosen quartz veins with a width/length ratio exceeding 1:5, so that veins behave as passive planes, with rotation approximating the bulk strain rate

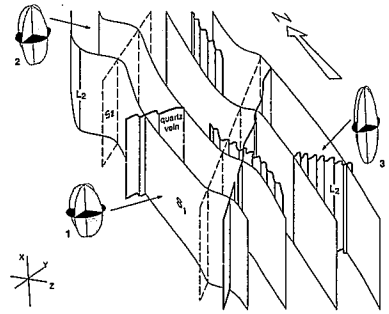
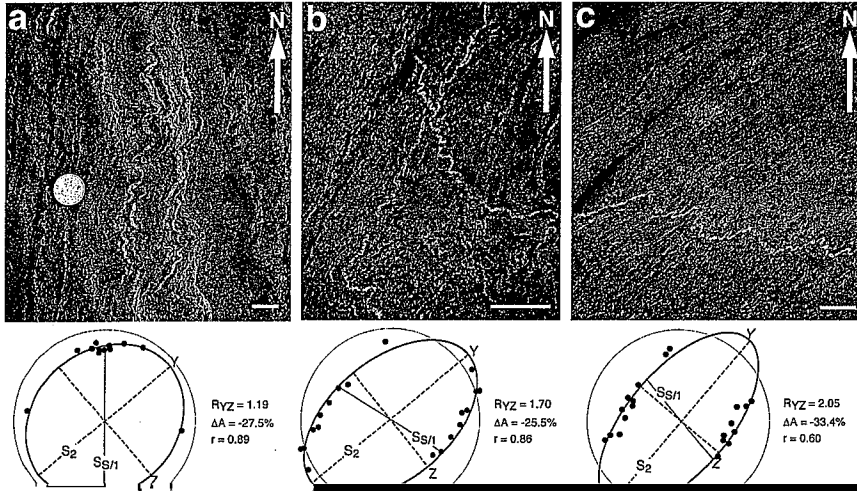


Fig. 3- Schematic block diagram showing the three-dimensional arrangement of the quartz veins used for strain analysis and their relationships with the main structural elements. 1, 2 and 3 are mean finite ellipsoids which respectively correspond to Q1 veins in long limbs, Q1 in short limbs and

vein type	position in the structure	rheology	X, Y, Z
Q1	long limbs	psammitic layers	1.26, 1.12, 0.71
Q1	long limbs	psammitic-pelitic alternances	1.49, 1.00, 0.67
Q1	short limbs and hinges	n.d.	1.63, 0.93, 0.66
Q2	n.d.	n.d.	2.15, 1.07, 0.43

Table 1: Mean values of the principal finite strain axis. n. d. = non differentiated.

Tabla 1: Valores medios de los ejes principales de la deformación finita. n. d. = no diferenciado.

ellipsoid for each locality. This has been made assuming constant volume, i. e. $XYZ = 1$, thus the length of the X axis is determined and the strain ratios for the other two principal finite strain planes.

Measurement errors represent a constraint of this method, specially when veins are measured in the extension field. Furthermore, the validity of the determined best-fit ellipsoids calculated by this method increases with increasing the dispersion in the orientation of quartz veins. This fact has represented a great limitation for the study case, since Q1 veins are mainly sub-parallel to $S_{s/1}$. The assumed constant volume has not been confirmed because the lack of veins with other attitudes than sub-vertical. However, volume changes should be negligible, considering the crystallinity of medium-high grade metamorphic rocks. The strain ellipsoid might be directly obtained without this limitation in orientation of the measured planar markers.

Discussion of the results

For each locality, a finite strain ellipsoid has been plotted using a polar diagram (Hsu 1966) with the strain intensity (ϵ_s , Nadai 1963) along the radial axis; and the strain shape (flattening vs. constrictional) measured by the Lode's parameter (v , Flinn 1978). These are respectively given by:

$$\epsilon_s = \left(\frac{2}{3}\right)^{1/2} \left[(\ln X/Y) + (\ln Y/Z) + (\ln X/Y)(\ln Y/Z) \right]^{1/2}$$

$$v = \frac{\ln Y/Z - \ln X/Y}{\ln Y/Z + \ln X/Y}$$

The results are shown in Fig. 4. Firstly, a marked higher ϵ_s is observed in ellipsoids corresponding to Q2 ($\epsilon_s > 1$) veins with respect to the obtained values from Q1 veins ($\epsilon_s < 1$). A possible explanation to this apparent contradiction points towards the role of mechanical anisotropy in controlling the different behaviour of Q1 (veins which are parallel to the $S_{s/1}$ anisotropy) and Q2 (veins cross-cutting the $S_{s/1}$) under the same bulk strain flow, i. e. part of Q1 vein deformation could be accommodated by layer-parallel shortening and shearing. The values of the finite strain ellipsoids for Q2 veins are inde-

pendent of the major structural pattern (decametric folds) and their average value is shown in table 1. In contrast, there is a structural control on the ellipsoids corresponding to the Q1 veins. In this way, the localities from long limbs give lower ϵ_s and flattening shape, whereas those from short limbs and hinge zones give higher ϵ_s and deviate to constrictional ellipsoids (Fig. 4). Another fact evidenced in this diagram is the rheological control in the partitioning of deformation, so that quartz vein in psammitic layers show lower ϵ_s than those in alternating psammitic-pelitic layers. These features are depicted with the different average values of the finite strain ellipsoids for Q1 (table 1 and Fig. 3).

An area loss of 37% in average in the YZ section has also been found. This area loss in the horizontal plane is consistent with the apparent extension in the vertical direction, if deformation isochoric. Because area decreasing in the ZY section, the field in the finite strain ellipse where veins have been shortened is larger than that where they have been extended. This explains why most measurable quartz veins have been folded or folded and boudinaged.

Conclusions

A strain analysis method based on the use of deformed quartz veins has been applied in the study area, allowing a quantitative estimation of finite strain. The diversity of the results is mainly due to:

(1) the two groups of quartz veins (Q1 and Q2) accommodated deformation in different ways and were differently influenced by the mechanical anisotropy.

(2) the heterogeneous character of the host rocks, giving rise to a rheological control in the partitioning of deformation, with quartz veins recording lower strains in the psammitic layers

(3) the inhomogeneous deformation in itself, causing a major structural pattern of asymmetric folds, with higher constrictional strains in the short limbs.

These quantitative estimations are rather consistent with field observations and

satisfy the previous interpretation of the regional structure, so that regional deformation in this area involved a 46% of vertical extension and 32% of horizontal shortening. In future studies, strain analysis could be focused on other strain markers in the area (such as competent layers intercalated in the metasedimentary sequence), which could give additional data to be contrasted with the present results. Furthermore, the analysis of asymmetric folding and/or boudinage structures in differently oriented quartz veins would furnish some new data concerning the vorticity of the flow.

Acknowledgements

The field work was financed by the D.G.I C.Y.T. PB 94-0685 project. Help, discussions and critical review from J. Carreras are much appreciated. We also thank A. Teixell for critically reading the text. The stereographic analysis was done with Stereonet, a program by R. W. Allmendinger.

References

- Carreras, J. and Casas, J. M. (1987): *Tectonophysics*, 135, 87-98.
- Carreras, J. and Druguet, E. (1994): *J. Struct. Geol.*, 16, 1525-1534.
- Druguet, E. (1997): *Unpubl. Thesis*, Univ. Autònoma de Barcelona.
- Druguet, E., Passchier, C. W., Carreras, J., Victor, P., and den Brok, S. (1997): *Tectonophysics*, 280, 31-45.
- Flinn, D. (1978): *J. Geol. Soc. London*, 135, 291-305.
- Gay, N. C. (1968): *Tectonophysics* 3, 81-88.
- Ghosh, S. K., and Ramberg, H. (1976): *Tectonophysics*, 34, 1-70.
- Hsu, T. C. (1966) *J. Strain Anal.*, 1, 216-222.
- Hutton, D. H. W. (1982): *J. Geol. Soc. London*, 139, 615-631.
- Kanagawa, K. (1990): *J. Struct. Geol.*, 12, 139-143.
- Nadai, A. (1963): *Theory of flow and fracture of solids*. McGraw-Hill. New York.
- Passchier, C. W. (1990): *Tectonophysics*, 180, 185-199.
- Ramsay, J. G. (1967): *Folding and fracturing of rocks*. Mc Graw Hill. New York. 568 p.
- Talbot, C. J. (1970): *Tectonophysics*, 9, 47-76.
- Talbot, C. J., and Sokoutis, D. (1995): *J. Struct. Geol.*, 17, 927-948.